44th AIAA/ASME/SAE/ASEE Joint Propulsion Conference & Exhibit
21 - 23 July 2008, Hartford, CT

AIAA 2008-5005

# The Role Of Current-Free Double-Layers In Plasma Propulsion

Eduardo Ahedo* and Manuel Martínez Sánchez †

*Massachusetts Institute of Technology, Cambridge, MA 02139, USA*

**Current free double layers are found in plasmas with two-temperature electron populations. A model of the expansion of this type of plasma in a Laval nozzle is presented. Stationary double layers form for a limited range of plasma parameters. They can be located either on the divergent nozzle, or the throat, or the convergent nozzle; in the two last cases, a non-neutral spatial rippling remain downstream of them. Relative gains in plasma propulsion parameters are found for moderately low values of hot electron density; gains tend to be larger when electrons are hotter and for larger nozzle expansion ratios. Both propulsion gains and double layer formation are associated to the anomalous thermodynamic properties of the plasma.**

## I. Introduction

Space plasma thrusters based on helicon sources are a subject of current large reserach.[1–6] A helicon-based thruster basically consists of a cylindrical helicon source where the plasma is produced and heated, and then, is expanded and accelerated into the vacuum. It is well known that during the expansion the plasma internal energy is transformed into a supersonic beam through the self-created ambipolar electric field.[7] Thus, no external electrode is needed to neutralize the current-free beam.

Charles and Boswell[3] have reported the formation of a current-free(CF) double-layer(DL), near the interphase of a helicon source tube and a larger diffusion chamber. Basically, a double layer consists of a positive and a negative Debye sheath, and connects two quasineutral regions of plasma. Because of its thinness, the double layer is observed as a jump in the profiles of the electric potential and the plasma density. Later, Charles and Boswell[8] detected ion beams with a large supersonic velocity (corresponding to a Mach number $\sim 2$), which agrees with a potential jump in the double layer, about 3-4 times larger than the plasma temperature in the source. This leads them to suggest the 'double layer helicon thruster' as an innovative and attractive propulsion device.

Although highly supersonic ion beams have been detected in other experiments with helicon sources,[9–11] the Charles-Boswell experiment is, as far as we know, the unique *direct* evidence of double layer formation in helicon sources. Furthermore, the double layer is observed only for high magnetic fields. In an experiment with lower magnetic fields (40-150G instead of the 270G of Ref. 3), Charles and Boswell[12] observe the formation of an ion beam for magnetic strengths above 50G, roughly. Although the authors claim this to be the transition to a DL regime, the profiles of plasma density they measure are perfectly smooth, with no sign of a double layer jump up to 150G.

In Ref. 12, the total fall of plasma density and the ion beam energy increase with the applied magnetic field. Hence these results would confirm the relevant role *of the magnetic field* in ion beam acceleration, through affecting the total fall of the quasineutral potential through the acceleration region. The benefits of a magnetic nozzle in improving beam acceleration were shown experimentally by Andersen et al.[13]

The current-free double layer is a particular case of double layers. The best known of these structures is the strong Langmuir double layer, which is characterized by (i) a potential fall much larger than the largest temperature of the surrounding quasineutral plasma, (ii) large non neutrality –i.e. relative charge density of the order of 100%–, and (iii) a large electric current from the low to the high potential side.[14–16]

*Professor, eduardo.ahedo@upm.es, AIAA Member. Permanent address: E.T.S. Ingenieros Aeronáuticos, Universidad Politécnica de Madrid, 28040 Madrid, Spain

†Professor, Department of Aeronautics and Astronautics, AIAA Member.

Current-free double layers (CFDL) have received attention in problems stemming from expansion of laser-produced plasma coronas[17–19] and material processing with electronegative plasmas.[20–22] In all these studies, the plasma is constituted by two negative species *with disparate temperatures*. The current-free double layer is formed only in a limited range of temperature and density ratios of the two negative species (making no difference whether these species are hot and cold electrons, or electrons and cold negative ions). A positive aspect is that there are only mild differences in CFDL conditions between fluid and kinetic models. If $\tau$ is the temperature ratio and $\alpha$ is the hot-to-total density ratio a current-free double layer forms for $\tau > 10$, roughly, and $\alpha$ relatively low.

Contrary to the Langmuir double layer, the current-free double layer is weak, in the sense that (i) the potential fall is smaller than the hot electron temperature, and (ii) the relative charge density is only a few percent. Steepened but fully quasineutral potential profiles are formed for parametric values close to those leading to a double layer formation. In this respect, it is worth noting that the distinction between a 'quasineutral region' and a 'non-neutral layer' has full sense only in the formal zero Debye length limit, i.e. $\lambda_D \ll L$ with $L$ the other characteristic length of the problem. This fact is more relevant in the case of the weak current-free double layer where the space-charge fields are not very large.

Hairapetian and Stenzel[23] ran an experiment of a collisionless expanding plasma with a controlled population of hot electrons; typical conditions were $\tau \sim 20$ and $\alpha \leq 5\%$. They demonstrated the direct relation between (a) the presence of a hot electrons and the steepening of the potential profile and (b) the hot electron temperature and the ion beam energy. The small space-charge density ($\sim 0.4\%$) and relatively large extension of the steepened region ($\sim 50 - 100$ Debye lengths) illustrate the unclear distinction, in practice, between a weak double layer and a mere steepened quasineutral profile.

The experiment of Hairapetian-Stenzel brings direct evidence that, as long as the plasma is collisionless in the acceleration region, the ion beam energy is determined by the total fall of the electric potential and this depends on the temperature and density of hot electrons. Whether the potential fall is more or less steepened, forming or not a double layer, is of marginal importance for ion acceleration.

Therefore, for propulsion applications, it is crucial to determine under which design and operation conditions a helicon-based thruster produces high energy electrons. Chen and Hershkowitz[24] have provided evidence of the generation of energetic electron beams in a steady helicon plasma discharge. They showed that the hot beam energy correlates with the wave phase velocity, and suggested electron trapping by the wave as the possible energizing mechanism.

This work presents a simple model of the acceleration of a three-species plasma through a Laval type nozzle (created most likely by the magnetic field). The objectives are to determine (i) the ion beam acceleration in terms of the nozzle expansion area and the plasma properties, (ii) the formation of intermediate double layers, and (iii) their relevance for propulsion applications.

The 'plasma acceleration' model makes two basic assumptions, which should be well satisfied in an efficient propulsion device. The first one is that the injected neutral gas is fully or almost-fully ionized upstream of the acceleration region. The second one is that for usual plasma parameters, the plasma is almost collisionless in the *short* acceleration region.

The rest of the paper is organized as follows. Section II presents the expansion model for a three-species plasma. Section III discusses fully quasineutral solutions. Section IV analyzes the formation of double layers in different locations of the plasma expansion. Section V, discusses propulsion coefficients and raises conclusions.

## II. Model of plasma expansion

We consider a fully-ionized, collisionless plasma, constituted by singly-charged ions ($i$) and 'cold'($c$) and 'hot'($h$) electron populations, which is accelerated electrostatically through a convergent-divergent, cylindrical nozzle characterized by its slowly-varying cross section $A(z)$. Pertinent macroscopic equations

are

$$An_iu_i = \text{const} = G_i, \tag{1}$$

$$\frac{1}{2}m_iu_i^2 + e\phi = 0, \tag{2}$$

$$n_e = n_c(\phi) + n_h(\phi), \qquad n_j = n_{j0}\exp\frac{e\phi}{T_j},\ (j = c, h), \tag{3}$$

$$\epsilon_0\frac{d^2\phi}{dz^2} = e(n_e - n_i), \tag{4}$$

where symbols are conventional. For the sake of clarity, the ion temperature (i.e the ion velocity dispersion) has been assumed small, $T_i \ll T_c$. The validity of the collisionless model relies on the condition

$$\nu_{ie}(u_i - u_e) \ll u_i^2 d\ln A/dz, \tag{5}$$

where $\nu_{ie}$ is the electron-to-ion collision frequency. The above condition is easily satisfied in practice if ionization is efficient: For an argon plasma of $10^{19}$ particles/m$^3$ and 5eV, one has $\nu_{ie} \sim 400\text{s}^{-1}$ and $u_i/\nu_{ie} \sim$ 9m, whereas plasma acceleration is expected to happen in a distance of the order of 1cm. The combination of confinement plus weak collisionality justifies the Maxwell-Boltzmann model selected for cold and hot electrons, instead of a polytropic one; quasi-Maxwellian distributions are implicitly assumed. The plasma will be quasineutral,

$$n_i = n_e \equiv n, \tag{6}$$

except where a non-neutral layer is formed. Observe that the current-free condition, $u_e = u_i$, with $u_e$ the effective axial velocity of electrons, is not an intrinsic part the model; this requires only that $u_e$ be small enough.

Considering the plasma as quasineutral fluid, thermodynamics properties can be defined in the usual way. Beyond their physical significance, these are useful for a comparison with a classical gas expansion through a Laval nozzle and for defining later propulsion parameters. Local pressure, temperature, and sound speed are

$$p_e = T_hn_h + T_cn_c, \qquad T_e = p_e/n_e, \qquad c_s = \sqrt{\frac{1}{m_i}\frac{dp_e}{dn_e}}, \tag{7}$$

respectively. Notice that the electrostatic potential plays the role of the specific enthalpy.[17]

Plasma expansion is going to depend on the nozzle expansion area,

$$\sigma = A_E/A_S, \tag{8}$$

with $A_S$ and $A_E$ the throat and exit sections of the nozzle, respectively. The nozzle walls are either physical or (more likely) magnetic flux surfaces, but this is outside the scope of the present work. For a magnetic nozzle, $\sigma$ is expected to be proportional to magnetic field strength and topology. Only for the purpose of depicting spatial plasma profiles, the nozzle profile

$$\frac{A(z)}{A_S} = \sigma - (\sigma - 1)\text{e}^{-z^2/L^2} \tag{9}$$

is used; here $L$ is the typical length scale of plasma acceleration, which is assumed much smaller than any collisional mean free path.

Dimensionless variables are

$$\bar{n}_{i,e} = \frac{n_{i,e}}{n_0}, \qquad \bar{u}_i = \frac{u_i}{\sqrt{T_c/m_i}}, \quad \psi = -\frac{e\phi}{T_c}, \quad \bar{G}_i = \frac{G_i}{A_Sn_0\sqrt{T_c/m_i}} \tag{10}$$

with $n_0 = n_{c0} + n_{h0}$. The dimensionless parameters determining plasma expansion are, on the one hand, the temperature and (upstream) densities ratios between the 2 electron populations:

$$\alpha = \frac{n_{h0}}{n_0}, \qquad \tau = \frac{T_h}{T_c}, \tag{11}$$

and the nozzle expansion area, $\sigma$.

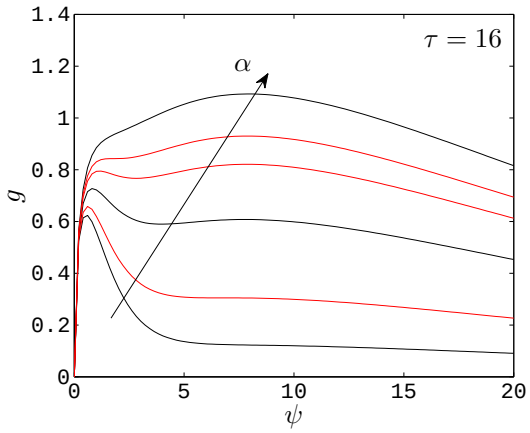


**Figure 1.** $g(\psi)$ **for** $\tau = 16$ **and increasing values of** $\alpha =$ **0.05, 0.125**($\alpha_1$) **, 0.25, 0.338**($\alpha_3$)**, 0.383**($\alpha_2$)**, and 0.45. Red lines correspond to transition values** $\alpha_1$**,** $\alpha_2$**, and** $\alpha_4$**.**

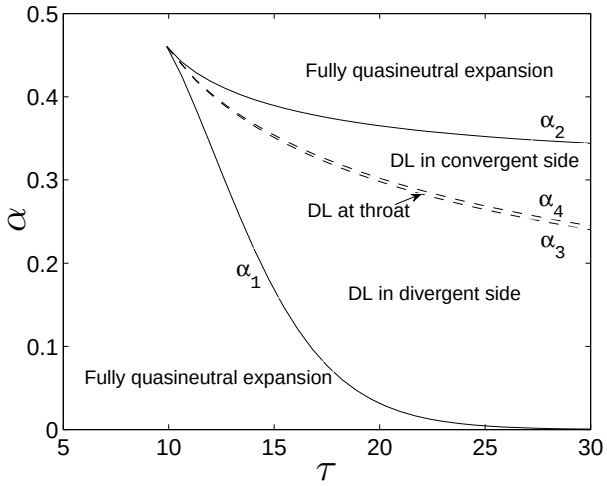


**Figure 2. Solid lines,** $\alpha_1(\tau)$ **and** $\alpha_2(\tau)$ **bound the region where double layers are formed inside the plasma. Dashed lines,** $\alpha_3(\tau)$ **and** $\alpha_4(\tau)$**, bound parametric regions with different locations within the nozzle of the double layer.**

## III. Fully quasineutral expansion

Equations (2) and (3) yield $\bar{n}_e(\psi)$ and $\bar{u}_i(\psi)$, which, combined, define the function

$$g(\psi) = \bar{n}_e \bar{u}_i = \sqrt{2\psi}\left[(1-\alpha)\mathrm{e}^{-\psi} + \alpha \mathrm{e}^{-\psi/\tau}\right]. \tag{12}$$

In any quasineutral region $g$ is the (dimensionless) ion flux, $\bar{n}_i \bar{u}_i$, which substituted in Eq. (1) yields an implicit equation for the potential profile $\phi(A(z))$:

$$g(\psi) = g_S \frac{A_S}{A(z)}, \tag{13}$$

where $g_S$ is the ion flux at the throat. The right-hand side of Eq. (13) presents a maximum at the nozzle throat. For the solution to be regular across that throat, $g(\psi)$ must be maximum there. For the global solution to be fully quasineutral $g(\psi)$ cannot present more extrema.

For a three-species plasma, $g(\psi)$ presents one or three local extrema depending on $\alpha$ and $\tau$,[17] as Fig. 1

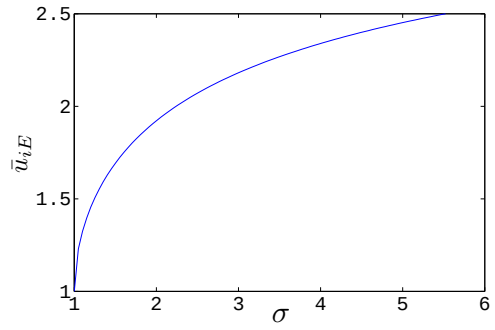


**Figure 3. Exhaust velocity of a two-species plasma versus nozzle expansion ratio.**

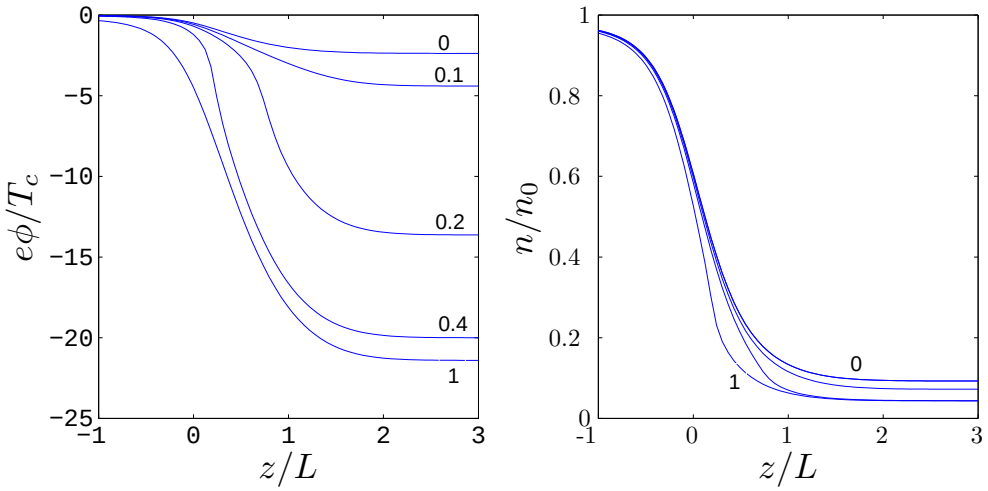


**Figure 4. Plasma profiles for $\tau = 9$, $\sigma = 3$ and several $\alpha$.**

illustrates. These extrema are the solutions of

$$0 = \frac{dg}{d\psi} = \frac{1}{\sqrt{2\psi}}\left[(1-\alpha)\mathrm{e}^{-\psi} + \alpha\mathrm{e}^{-\psi/\tau}\right] - \sqrt{2\psi}\left[(1-\alpha)\mathrm{e}^{-\psi} + \frac{\alpha}{\tau}\mathrm{e}^{-\psi/\tau}\right], \tag{14}$$

which is just the condition that $u_i$ is sonic. There is a single maximum for any $\alpha$ if $\tau$ is below the threshold value $\tau^* = 5 + \sqrt{24} = 9.90$. For larger $\tau$, there are two maxima and no fully quasineutral plasma expansion exists within an interval $\alpha_1(\tau) < \alpha < \alpha_2(\tau)$, which is depicted in Fig. 2; lines $\alpha_3(\tau)$ and $\alpha_4(\tau)$ in that figure are defined later. The two maxima of $g$ are located at $-e\phi \sim T_c/2$ and $-e\phi \sim T_h/2$.

Within the parametric region of a single maximum, Eqs. (12) and (14) determine $\psi_S(\tau,\alpha)$ and $g_S(\tau,\alpha)$ and the problem is solved. For the simple case of a single electron population of temperature $T_c$ (i.e. for $\alpha = 0$), one has

$$\psi_S = 1/2, \quad g_S = 1/2\sqrt{\mathrm{e}}, \tag{15}$$

(Clearly, for $\alpha = 1$, we just have to exchange $T_c$ by $T_h$.) Then, the solution is just a simple subsonic/supersonic plasma expansion with a sonic velocity $u_{iS} = \sqrt{T_c/m_i}$ at the nozzle throat. The total fall of electric potential and plasma density, and, therefore, the ion velocity at the nozzle exit, $u_{iE}$, grow with the nozzle expansion area, as Fig. 3 illustrates.

The changes on plasma expansion profiles when a second electron population exists are illustrated in Fig. 4, for a value of $\tau$ slightly below $\tau^*$. As $\alpha$ increases from zero the overall potential drop and beam energy increase, which is natural since the energy stored in the upstream plasma increases too. Nonetheless, there are several interesting, non-obvious features related to $\alpha \sim \alpha_1(\tau^*) \simeq 0.46$. First, the increase in ion beam energy is not linear with $\alpha$: there is almost no increase for $\alpha > 0.46$, so that similar ion beam energies

are obtained with 40% and 100% of hot electrons. Second, the steepening of the potential profile is maximum (i.e. maximum ambipolar electric field) for $\alpha \sim 0.46$. And third, the potential at the sonic point (relative to the upstream plasma) changes from $\sim T_c/2e$ to $\sim T_h/2e$ at $\alpha \sim 0.46$.

## IV. Expansion with an intermediate double layer

For $(\tau, \alpha)$ in the region $\tau > \tau^*$ and $\alpha_1(\tau) < \alpha < \alpha_2(\tau)$, a double layer is expected to connect two quasineutral regions with regular potential profiles, that is without turning points. The double layer can be placed either in the convergent or divergent side of the nozzle. Consider, for instance, the case $\tau = 16$ depicted in Fig. 1. For $\alpha$ slightly above $\alpha_1 \simeq 0.125$, continuity considerations suggest that point S is at the first maximum of $g(\psi)$ and the double layer is located in the divergent nozzle (i.e. $\psi > \psi_S$). On the contrary, for $\alpha$ slightly below $\alpha_2 \simeq 0.383$, the second maximum of $g(\psi)$ is expected to still define throat conditions (i.e. point S) and the double layer to be placed in the convergent nozzle (i.e. $\psi < \psi_S$). Next, we analyze the characteristics of these double layers and then discuss the whole plasma expansion. Double layers structures are not going to be identical in the convergent and divergent sides of the nozzle: the *simple*, monotonic double layer is going to exist only on the divergent nozzle.

### A. Double layer in the divergent nozzle

The plasma behavior inside the double layer is obtained by applying the asymptotic limit $\lambda_D/L \to 0$ to plasma equations (1)-(4) and solving the resulting Poisson equation,

$$\frac{d^2\psi}{d\xi^2} = \bar{\rho}(\psi), \qquad \bar{\rho} = \bar{n}_i(\psi) - \bar{n}_e(\psi); \tag{16}$$

here $\xi = (x - x_{DL})/\lambda_D$ is the inner spatial variable, with $x_{DL}$ any point inside the double layer and $\lambda_D = \sqrt{\epsilon_0 T_c/e^2 n_0}$. A first integral of the Poisson equation is

$$\frac{1}{2}\left(\frac{d\psi}{d\xi}\right)^2 = \int \bar{\rho}(\psi) d\psi \equiv U(\psi) + \text{const}, \tag{17}$$

where the function $U(\psi)$ is known as the (dimensionless) Sagdeev's potential.

The formation of a double layer inside any plasma requires the following three conditions at *both* two boundaries, A and B:[15,16]

(a) Plasma quasineutrality;

(b) The space-charge field becomes zero (asymptotically) (in order to match with the much-weaker ambipolar field of the quasineutral regions); and

(c) The beam-like species (ions in our case) must be sonic or supersonic, in order the double layer develops a (spatially) non-oscillatory, space-charge potential. This is called the Bohm condition. [This condition is not going to be satisfied in one case, leading to a double layer with a rippled potential tail.]

These conditions imply that the constant in Eq. (17) is $-U_A$ and

$$U'_A = 0, \qquad U'_B = 0, \qquad U_B = U_A, \qquad U''_A \geq 0, \qquad U''_B \geq 0. \tag{18}$$

For our three-species plasma, the dimensionless electric charge is

$$\bar{\rho}(\psi) = \frac{g_A}{\sqrt{2\psi}} - \bar{n}_c(\psi) - \bar{n}_h(\psi), \tag{19}$$

with $g_A$ the ion flux at the double layer entrance, and their integral –the Sagdeev's potential– can be expressed as

$$U(\psi; \alpha, \tau, g_A) = \sqrt{2\psi} g_A + \bar{n}_c(\psi) + \tau \bar{n}_h(\psi). \tag{20}$$

Then, it is easy to find that, in terms of function $g$, boundary conditions (a) and (c) imply that

$$g_A = g_B, \qquad g'_A \leq 0, \qquad g'_B \leq 0. \tag{21}$$

Therefore, a standard double layer connects horizontally two points of the flux function $g(\psi)$ *with non-positive slopes necessarily*. Finally, condition (b), $U_B = U_A$, determines univocally the location of points A and B of the double layer.

Applying these conditions, it turns out that the double layer is located in the divergent nozzle for $\tau > \tau^*$ and $\alpha_1(\tau) < \alpha < \alpha_3(\tau)$, as shown in Fig. 1. At $\alpha = \alpha_3$ the double layer location reaches the nozzle throat, with sonic conditions being reached at the DL upstream boundary A.

Figure 5 shows the potential and density profiles inside a double layer placed at the divergent nozzle. Observe that cold electrons are strongly confined by the double layer, and are practically absent downstream of it. The potential jump across the double layer, $\phi_{AB} \equiv \phi_B - \phi_A$, is large in terms of $T_c$ but relatively small in terms of $T_h$: $e\phi_{AB} \sim T_h/2$, which indicates that the double layer is weak. A more evident indication is the small value of the electric charge, $\rho$, no larger than 5% of $n_i$. A third indication is the DL extension, of the order of tens of Debye lengths. These characteristics agree with the experimental ones of Hairapetian and Stenzel.[23] For a given $\tau$, the double layer located at the nozzle throat presents the largest potential jump.

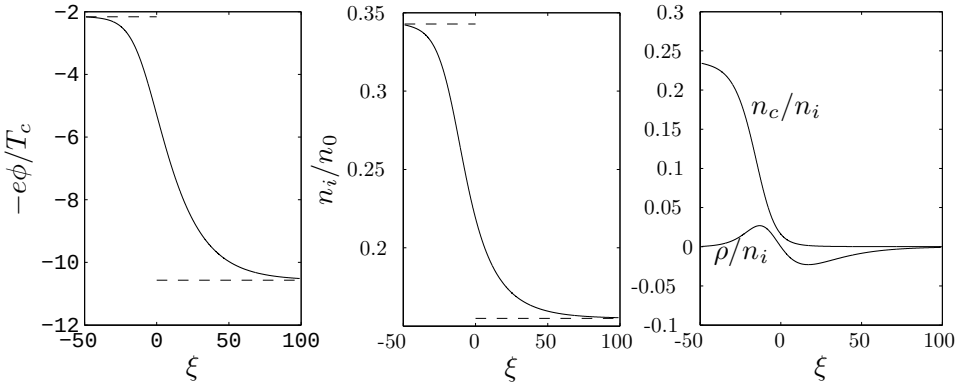


**Figure 5. Internal structure of a double layer placed in the divergent side, for $\tau = 16$ and $\alpha = 0.30$. Dashed lines are the values at the boundaries A and B.**

### B. Double layer in the convergent nozzle

Let H1, H2, and L be the locations of the first maximum, second maximum, and the intermediate minimum of of $g(\psi)$, respectively. For $\alpha > \alpha_2$, there exists H2 only and the sonic point S is located there. When $\alpha$ becomes lower than $\alpha_2$, the maximum H1 and the minimum $L$ appear; for $\alpha$ near $\alpha_2$, we expect point S to remain at H2 and a double layer to develop around H1 and L, in the convergent nozzle. However, conditions on the slope of $g$, related to the Bohm conditions, make it impossible to place a *simple* double layer there. First, the boundary A cannot be to the left of point H1, since there the slope of $g$ is positive, violating Eq. (21). Second, point A cannot be to the right of point H1, since then there would be a turning point of plasma profiles at point H1. Hence, the only possibility is that point A is located at H1. Let us now try to place point B, either to the right of H2, or between L and H2. The first possibility is satisfied only for $\alpha = \alpha_3(\tau)$, which corresponds to the transition case of the previous subsection. The second possibility violates again Eq. (21).

The consequence is that at least one of the conditions defining a double layer must be relaxed and a more complex non-neutral layer is formed. If the sonic point is assumed to be placed at point H2, point H1 is necessarily the transition point A to a non-neutral layer. Then, solving Poisson equation from point A, with $U'_A = 0$ and $U''_A = 0$, a point C (to the right of L) is reached where the space-charge field becomes zero, (i.e. $U_C = U_A$) but the electric charge is negative, $\rho_C < 0$. Therefore, point C *does not* connect to a quasineutral region. Instead, this point C connects to a second-non-neutral region, characterized by a spatial rippling of the electric potential (with $\phi_C < \phi < \phi_D$) and other plasma magnitudes. In order to determine the maximum potential in this rippled region there, $\phi_D$, the barrier effect on electrons of the minimum potential at C must be taken into account. After the first point C the electron density in the rippled region does not follow Eq. (3) but it is constant, $n_e = n_{eC}$, as can be derived easily from the modified velocity distribution function. This changes the Sagdeev's potential in the rippled region, which becomes

$$U_m(\psi, g_A, n_{eC}) = \sqrt{2\psi} g_A - n_{eC}\psi. \tag{22}$$

Then, the zero electric field condition,

$$U_m(\psi_C) = U_m(\psi_D), \tag{23}$$

determines the potential at point D. Figure 6 shows an example of this monotonic-plus-rippled non-neutral region. Observe again the small charge density and the strong screening of cold electrons from the downstream side.

This type of structure is well known in studies of current-free double layers. Indeed, our model *in the convergent side of the nozzle* is practically identical to the one considered by Kono[21] in the context of the interaction of a wall with an electronegative plasma in a (spherically) convergent geometry. In that problem, the sonic point S is the (*singular*) transition to the Debye-sheath around the wall instead of the (*regular*) transition in the nozzle throat to the divergent side. Furthermore, in terms of plasma acceleration, Kono's problem is analogous to the Tonks-Langmuir problem with a three-species plasma, treated, for instance, by Sheridan et al.[22] In this last case, plasma ionization, instead of a convergent geometry, is the mechanism leading to the creation of ambipolar electric field that accelerates the plasma. Both Kono and Sheridan et al. find a *double layer with a downstream rippled boundary.*

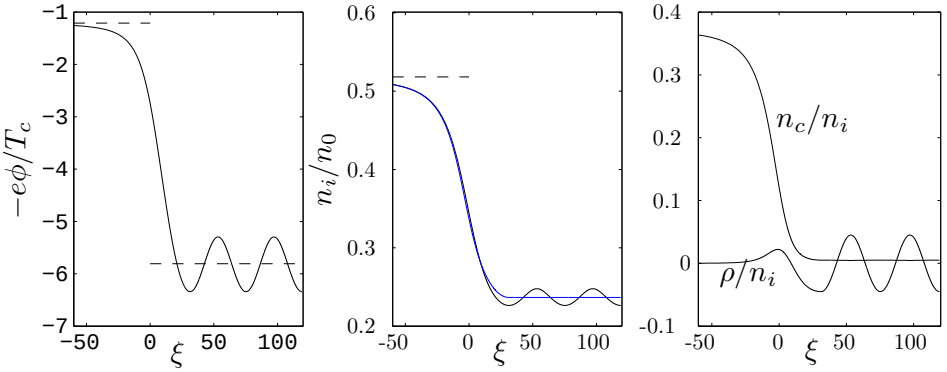


**Figure 6. Internal structure of a double layer placed in the convergent side, for $\tau = 16$ and $\alpha = 0.35$. In the central plot $n_i$ and $n_e$ are in black and blue, respectively. Dashed lines are the values at the boundaries A and B.**

Coming back to our problem, there remains the issue of connecting the downstream rippled region of scale $\lambda_D$ with the quasineutral plasma of scale $L$. A first way to do it is to take $\lambda_D/L$ finite and to solve the full non-neutral model numerically. This last procedure was followed both by Kono and Sheridan et al., and confirmed the development of a monotonic double layer around point H1, followed by a two-scale plasma profile consisting of a space-charge rippling plus a smooth variation. A second exact way is to apply, downstream of (first) point C, an asymptotic two-scale analysis.[25] On the one hand, this is cumbersome and we expect the rippling to be small and the space-charge to cancel out over several periods. On the other hand, the physical significance of the spatial rippling is unclear since occasional collisional processes would create trapped particles, that tend to diminish the rippling.[21]

Hence, we opt here for finding a solution that averages out the small rippling downstream of the monotonic non-neutral subregion. This requires us to choose a condition to define the quasineutral downstream boundary (which will continue to be named point B) of the monotonic 'double layer'. The appropriate choice is

$$n_B = n_{eC}, \tag{24}$$

which yields $u_{iB} = g_A/n_B$ and $\psi_B = 2u_{iB}^2$. The small potential barrier on electrons requires some adjustment of the electron Maxwell-Boltzmann laws in Eq. (3). Thus, downstream of point B one has

$$\bar{n}_e(\psi) = (1-\alpha)\mathrm{e}^{-\psi+\psi_B-\psi_C} + \alpha\mathrm{e}^{-(\psi+\psi_B-\psi_C)/\tau}, \tag{25}$$

which affects the expression of $g(\psi)$, Eq. (12), downstream of point B.

This solution with a double layer and no-rippling of plasma profiles turns out to be very satisfactory since it covers the region $\tau > \tau^*$, $\alpha_3 < \alpha < \alpha_2$ and therefore completes the analysis of the problem in the parametric plane $(\tau, \alpha)$. At the same time, two subregions are distinguishable in terms of the location of the double layer, which are separated by a line $\alpha = \alpha_4(\tau)$, Fig. 2: for $\alpha_4 < \alpha < \alpha_2$, the double layer is located in the convergent nozzle; for $\alpha = \alpha_4$, the DL is located at the nozzle throat with the sonic point coinciding with the downstream boundary B; and, for $\alpha_3 < \alpha < \alpha_4$, the double layer remains in the throat, with the sonic point moving from point B to point A, thus providing the desirable continuity with the DL solution

found in the previous subsection. It is in the thin region $\alpha_3 < \alpha < \alpha_4$ where the sonic potential, $\phi_S$, changes from $\sim -T_c/2e$ to $\sim -T_h/2e$

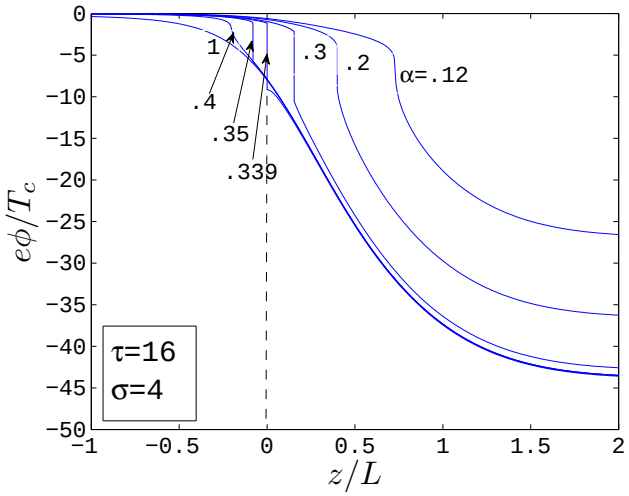


**Figure 7. Plasma profiles for $\tau = 16$ and $\sigma = 4$, with and without intermediate double layers. The nozzle throat is at $z = 0$.**

### C. Quasineutral profiles with double layers

Figure 7 illustrates, for $\tau = 16$, the changes on plasma profiles and double layer characteristics with $\alpha$, covering the five different regimes:

a) low temperature quasineutral expansion, for $\alpha < \alpha_1$,
b) expansion with double layer in divergent side, for $\alpha_1 < \alpha < \alpha_3$,
c) expansion with double layer in the nozzle throat, for $\alpha_3 < \alpha < \alpha_4$,
d) expansion with double layer in convergent side, for $\alpha_4 < \alpha < \alpha_2$,
e) high temperature quasineutral expansion, for $\alpha_2 < \alpha$,

with $\alpha_1 \simeq 0.1249$, $\alpha_3 \simeq 0.3379$, $\alpha_4 \simeq 0.3412$, and $\alpha_2 \simeq 0.3829$.

We find that, in the quasineutral scale, plasma profiles for $\tau < \tau^*$ evolve similarly with $\alpha$ than those for $\tau < \tau^*$. The main difference, in a two-scale analysis, is the presence of a discontinuity instead of a steepened variation, but even that difference becomes diluted for, say, $\lambda_D/L > 10^{-2}$. Furthermore, except for a small nozzle expansion ratios, the DL potential fall does not constitute most of the total potential fall in the nozzle. The maximum potential jump across the DL is found for $\alpha = \alpha_3$.

## V. Propulsion coefficients and conclusions

For propulsion considerations, the relevant parameters are thrust and specific impulse (in velocity units),

$$F = G_i m_i u_{iE} + p_{eE} A_E, \qquad I_{sp} = F/m_i G_i, \tag{26}$$

respectively, which depend on the ion flow $G_i$ and the exhaust velocity $u_{iE}$. In order to compare, *for the same nozzle*, the propulsive characteristics of different plasmas, and, in particular, *propulsive gains* associated to the presence of hot electrons or double layers, dimensionless parameters need to be defined. Usual parameters, such as partial efficiencies, cannot be defined because the present model is limited to an *ideal* nozzle expansion with no consideration of plasma ionization and heating, on the one hand, and downstream expansion, on the other hand.

Therefore, propulsion characteristics will be measured with the two following dimensionless parameters:

$$C_F = \frac{F}{p_{e0} A_S}, \qquad C_I = \frac{I_{sp} g_0}{\sqrt{T_{e0}/m_i}}. \tag{27}$$

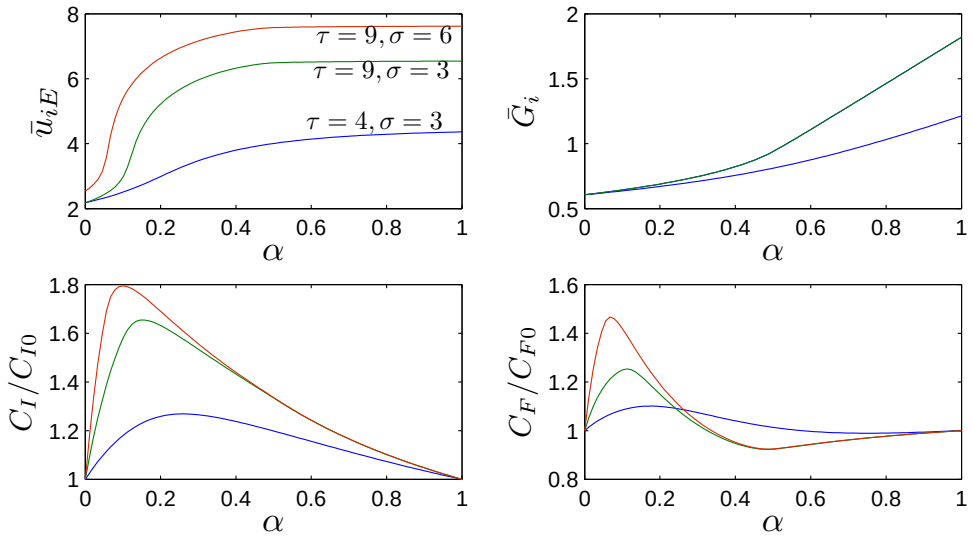


**Figure 8. Propulsion parameters for a three-species plasma versus $\alpha$ for several values of $\tau$ and $\sigma$; $\bar{G}_i$ is independent of $\sigma$.**

with subindices 0 meaning upstream values. The first parameter is the usual thrust coefficient;[26] the second one is a specific-impulse coefficient, which compares the exhaust velocity versus the upstream sound speed based on $T_e$; $C_F/C_I$ would be the plasma flow parameter. These two coefficients screen off the obvious dependence of $F$ and $I_{sp}$ on the plasma specific energy upstream of the nozzle and therefore give a measure of the 'specific propulsive capacity' of the plasma. For a simple, two-species plasma, these two coefficients (called $C_{I0}$ and $C_{F0}$) depend only on the nozzle expansion coefficient, $\sigma$; see Fig. 3 for the main contribution to $C_{I0}$.

Figures 8 and 9 show the variation of propulsion parameters with $\alpha$ for plasmas with $\tau = 9$ and 16, respectively. For $\tau = 16$, we can observe, at $\alpha \sim \alpha_3 \sim 0.339$, the effect of the quick change in throat conditions when the double layer is anchored to it. Both $\bar{u}_{iE}$ and $\bar{G}_i$ depend on the plasma energy and therefore increase monotonically with $\alpha$ and $\tau$; $\bar{u}_{iE}$ increases with $\sigma$ too. The interesting feature, already commented before, is that, for given $\tau$ and $\sigma$, $\bar{u}_{iE}$ does not grow proportionally to $\alpha$: most of the increment occurs at low $\alpha$. This effect is more pronounced as $\tau$ increases. Indeed, for $\tau > \tau^*$, $\bar{u}_{iE}|_{\alpha=1}$ is reached, in practice at $\alpha = \alpha_3$. The plasma flow function $\bar{G}_i(\alpha)$ presents two slopes, which are proportional to the two typical magnitudes of the ion sound speed, that is to $T_c^{1/2}$ and $T_h^{1/2}$.

In order to compare better with the simple, two-species plasma and to shield out partially the influence of $\sigma$, relative propulsion coefficients $C_I/C_{I0}$ and $C_F/C_{F0}$ have been plotted in Figs. 8 and 9. In this way, whenever these coefficients are larger than one it can be said that a three-species plasma presents a propulsive gain over a two-species plasma. The conclusions from the figures are rather interesting:

First, a three-species plasma brings always a gain in specific impulse. For given $\tau$ and $\sigma$, the gain is maximum at a moderately low value of $\alpha$. To be definite, let us compare the cases $\alpha = 0$ and $\alpha = 0.11$, both with $\tau = 9$ and $\sigma = 6$, that is both with no DL formation. For the same upstream plasma density $n_0$, the internal energy of the second plasma is twice the energy of the first simple plasma. If specific impulse would depend only on the (square root) of the internal energy, it would be 1.4 times higher for the second plasma; instead it is 2.5 times larger, meaning a relative gain of 80%.

Second, the maximum gain increases with $\tau$ and $\sigma$, that is by either creating hotter electrons, or increasing the nozzle expansion area. In the case of a magnetic nozzle, the second possibility means to increase the magnetic strength. The first way, hotter electrons, was proven by Hairapetian and Stenzel.[23] The second way was, in fact, proven by Charles and Boswell in Ref. 12.

Third, gains or losses are found on the relative thrust coefficient, $C_F/C_{F0}$, depending on $\alpha$, $\tau$, and $\sigma$. Losses come basically from the concave behavior of $\bar{G}_i(\sigma)$ –or $C_G = C_F/C_I$–, that is from a certain flux reduction in a three-species plasma at intermediate values of $\alpha$. For instance, for the two plasmas commented above, the flux of the case $\alpha = 0.11$, is 2/3 of that for $\alpha = 0$. Still, thanks to the large gain in specific

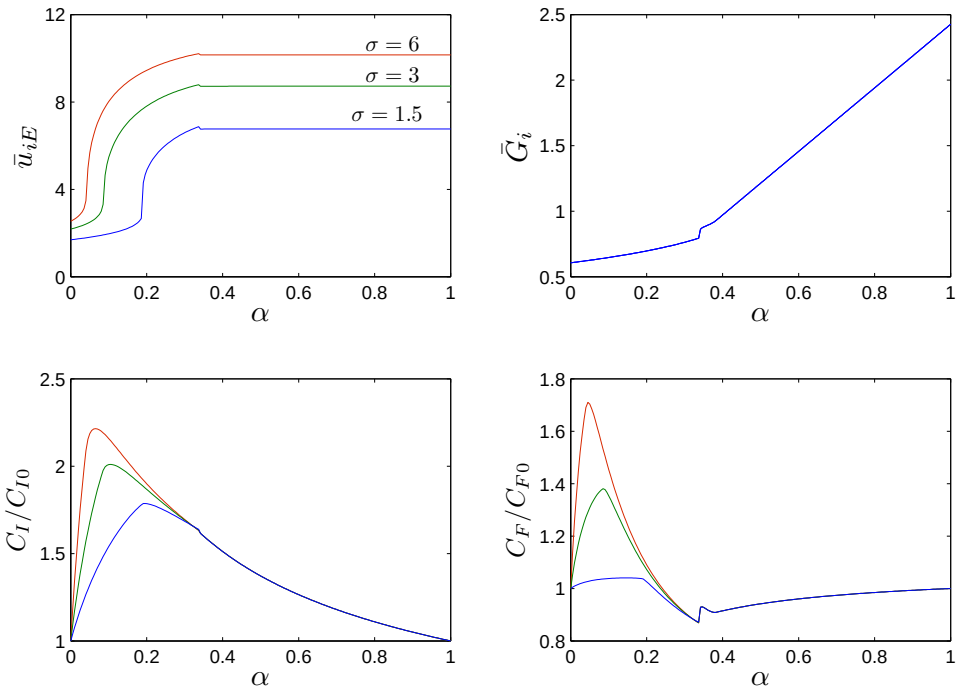


**Figure 9. Propulsion parameters for a three-species plasma versus $\alpha$ for $\tau = 16$ and several $\sigma$. $\bar{G}_i$ is independent of $\sigma$.**

impulse, there is a 40% relative gain in thrust.

Finally, all the analysis leads us to conclude that the gains in specific impulse and beam specific power in a three-species plasma are independent of the presence of a double layer. The gains are due to the anomalous thermodynamic behavior created by the presence of hot electrons in the plasma. The DL formation has no role in the propulsion gain, it is only another consequence of these thermodynamic effects.

## Acknowledgments

The work of E. Ahedo was financed by the Ministerio de Ciencia e Innovación of Spain, under Project ESP2007-62694.

## References

[1]F. R. Chang Diaz, J. P. Squire, R. D. Bengtson, B. N. Breizman, F. W. Baity, and M. D. Carter. The Physics and Engineering of the VASIMR Engine. In *36th Joint Propulsion Conference, Huntsville, Alabama*, AIAA 2000-3756. American Institute of Aeronautics and Astronautics, Washington DC, 2000.

[2]K. Toki, S. Shinohara, T. Tanikawa, I. Funaki, and K.P. Shamrai. Preliminary Investigation of Helicon Plasma Source for Electric Propulsion Applications. In *28th International Electric Propulsion Conference, Toulouse, France*, IEPC 2003-0168. Electric Rocket Propulsion Society, Fairview Park, OH, 2003.

[3]C. Charles and R. Boswell. Current-free double-layer formation in a high-density helicon discharge. *Applied Physics Letters*, 82(9):1356–1358, 2003.

[4]T. Ziemba, J. Carscadden, J. Slough, J. Prager, and R. Winglee. High Power Helicon Thruster. In *41th Joint Propulsion Conference, Tucson, AR*, AIAA 2005-4119. American Institute of Aeronautics and Astronautics, Washington DC, 2005.

[5]J. M. Pucci, N. Sinenian, J. Palaia, M. Celik, Z. LaBry, A. Shabshelowitz, O. Batishchev, and M. Martínez-Sánchez. Preliminary Characterization of a Helicon Plasma Source for Space Propulsion. In *42th Joint Propulsion Conference, Sacramento, CA*, AIAA 2006-5255. American Institute of Aeronautics and Astronautics, Washington DC, 2006.

[6]K.P. Shamrai, Y.V. Virko, V.F. Virko, and A.I. Yakimenko. Compact Helicon Plasma Source with Permanent Magnets for Electric Propulsion Application. In *42th Joint Propulsion Conference, Sacramento, CA*, AIAA 2006-4845. American Institute of Aeronautics and Astronautics, Washington DC, 2006.

[7]A.V. Gurevich, L.V. Pariiskaya, and L.P. Pitaevskii. Self-similar Motion of Rarefied Plasma. *Soviet Physics JETP*, 22:449–, 1966.

[8]C. Charles and R. Boswell. Laboratory evidence of a supersonic ion beam generated by a current-free 'helicon' double-layer. *Physics of Plasmas*, 11:1706–1714, 2004.

[9]S. A. Cohen, N. S. Siefert, S. Stange, R. F. Boivin, E. E. Scime, and F. M. Levinton. Ion acceleration in plasmas emerging from a helicon-heated magnetic-mirror device. *Physics of Plasma*, 10:2593–2598, 2003.

[10]X. Sun, C. Biloiu, R. Hardin, and E. E. Scime. Parallel velocity and temperature of argon ions in an expanding, helicon source driven plasma. *Plasma Sources Sci. Technol.*, 13:359–370, 2004.

[11]R. Walker, N. Plihon, P. Chabert, and J.-L. Raimbault. Experimental Studies of Helicon Double Layers for Future High Power Plasma Propulsion. In *42th Joint Propulsion Conference, Sacramento, CA*, AIAA 2006-4844. American Institute of Aeronautics and Astronautics, Washington DC, 2006.

[12]C. Charles and R. W. Boswell. The magnetic-field-induced transition from an expanding plasma to a double layer containing expanding plasma. *Applied Physics Letters*, 91:201505, 2007.

[13]S. A. Andersen, V. O. Jensen, P. Nielsen, and N. D'Angelo. Continuous Supersonic Plasma Wind Tunnel. *Phys. Fluids 12*, 12:557–560, 1969.

[14]I. Langmuir. The interaction of electron and positive ion space charges in cathode sheaths. *Physical Review*, 33:954–, 1929.

[15]L.P. Block. A double layer review. *Astrophysics and Space Science*, 55:59–83, 1978.

[16]M. A. Raadu. The physics of double layers and their role in astrophysics. *Physics Reports*, 178:26–97, 1989.

[17]B. Bezzerides, D. W. Forslund, and E. L. Lindman. Existence of rarefaction shocks in a laser-plasma corona. *Phys Fluids*, 21:2179–2186, 1978.

[18]L. M. Wickens, J. E. Allen, and P. T. Rumsby. Ion Emission from Laser-Produced Plasmas with Two Electron Temperatures. *Phys. Rev. Lett.*, 41:243 – 246, 1978.

[19]A. Gurevich, D. Anderson, and H. Wilhelmsson. Ion Acceleration in an Expanding Rarefied Plasma with Non-Maxwellian Electrons. *Phys. Rev. Lett.*, 42:769–772, 1979.

[20]K. Sato and F. Miyawaki. Formation of presheath and current-free double layer in a two-electrontemperature plasma. *Physics of Fluids B*, 4(5):1247–1254, 1992.

[21]A. Kono. Formation of an oscillatory potential structure at the plasma boundary in electronegative plasmas. *J. Phys. D: Appl. Phys.*, 32:1357–1363, 1999.

[22]T. E. Sheridan, P. Chabert, and R. W. Boswell. Positive ion flux from a low-pressure electronegative discharge. *Plasma Sources Sci. Technol.*, 8:457–462, 1999.

[23]G. Hairapetian and R. L. Stenzel. Particle dynamics and current-free double layers in an expanding, collisionless, two-electron-population plasma. *Physics of Fluids B*, 3(4):899–914, 1991.

[24]R. T. S. Chen and N. Hershkowitz. Multiple Electron Beams Generated by a Helicon Plasma Discharge. *Physical Review Letters*, 80:4677–4680, 1998.

[25]C. M. Bender and S. A. Orszag. *Advanced Mathematical Methods for Scientists and Engineers*. Mc Graw-Hill, Singapore, 1986.

[26]G.P. Sutton and O. Biblarz. *Rocket Propulsion Elements, 7th edition*. Wiley, New York, 2001.